Hearing Research 468 (2025) 109377

Contents lists available at ScienceDirect

Hearing Research

journal homepage: www.elsevier.com/locate/heares

Research Paper

Colossal ears? How baleen whales hear low-frequency sound

Ted W. Cranford [a,*], Margaret A. Morris [b], Petr Krysl [c], John A. Hildebrand [b]

[a] Department of Biology, San Diego State University, San Diego, 92182, USA
[b] Scripps Institution of Oceanography, University of California, San Diego, 92093, USA
[c] Department of Structural Engineering, University of California, San Diego, 92093, USA

ARTICLE INFO

Keywords:
Mysticete audition
Bone conduction hearing
Low-frequency sound
Tympanoperiotic complex (TPC)
Baleen whales
Amplified hearing
Mechanical amplification
Long distance signaling

ABSTRACT

Baleen whales produce and receive underwater sounds with wavelengths much longer than their bodies, despite having ears approximately the size of a human fist. How do they hear long wavelength sounds with relatively small ears? In 2015, we produced a computational model to simulate low-frequency hearing in the fin whale. That study predicted bone conduction as the most likely hearing mechanism. The whale's enormous skull acts as an external ear, capturing sounds like an acoustic antenna and transmitting them to other parts of the ear.

In the current study, we tested the bone conduction hypothesis with physical, vibroacoustic experiments using partially denuded gray whale skulls. These experiments *validated* that long wavelength sounds excite skull vibrations, which are amplified and transferred to the dynamic components of each bony ear, known as the tympanoperiotic complex. Vibrations of the dynamic components include the bony pedicles, tympanic bullae and middle ear ossicles, resulting in displacement of fluid within the cochlea of the inner ear.

The pedicles are important components of this mechanism, thin flexible bones that suspend the bullae from the periotic, amplifying the low-frequency vibrations from the skull. We contend that this skull-driven pathway of sound reception and amplification within the bony ear complexes is key to understanding low-frequency hearing capabilities and mysticete natural history.

1. Introduction

Filter-feeding mysticete whales are oceanic giants. The means by which baleen whales hear low-frequency sounds are essential to their survival. Their hearing mechanisms enable them to sense the environment, engage in long-distance signaling for communication, and maintaining social cohesion (Payne, 1995; Tyack, 1997; Clark and Ellison, 2004, 2022).

Blue whale (*Balaenoptera musculus*) with researcher Bruce Mate on a boat attempting to attach a satellite tag, Santa Barbara, California - Flip Nicklin/ Minden Pictures.

---

* Corresponding author.
E-mail address: tcranfor@sdsu.edu (T.W. Cranford).

https://doi.org/10.1016/j.heares.2025.109377
Received 3 April 2025; Received in revised form 28 June 2025; Accepted 23 July 2025

Mysticetes produce a broad range of low-frequency (LF) vocalizations (Edds-Walton, 1997; Brownell et al., 2008) and their auditory systems have presumably evolved to include these frequencies. The long wavelengths of the lowest frequency sounds produced by these whales can exceed multiple body lengths. Paradoxically, Groves and colleagues reported that the tympanic bullae in the largest mysticetes are proportionally the smallest when compared to body size (Groves et al., 2021), but they did not consider the potential role of the entire skull as an integral part of the hearing apparatus, functionally the external ear.

We begin with a brief introduction to the basic anatomic structure of the mysticete auditory system, followed by an outline of the bone conduction hypothesis. Next, we present a synopsis of validated evidence demonstrating that hearing in mysticetes is mechanically driven and amplified by a system of cranial bones connected by ligaments (Cranford and Krysl, 2015; Morris et al., 2025). Finally, we discuss the implications derived from bone conduction hearing for various aspects of mysticete natural history.

The mysticete auditory system includes the entire skull and bilateral bony ear complexes (Fig. 1). Each bony tympanoperiotic complex (TPC) is firmly attached to the skull. The interactions between the whale's skull and long wavelength sounds in the ocean, forces the skull into motion. These vibrations are then transmitted to the bony TPCs. This bone conduction mechanism is similar to notions concerning atympanic hearing in animals, such as early tetrapods, or humans (bone conduction hearing).

In Fig. 1, the skull and TPCs are components of the mysticete auditory apparatus, while the mandibles and the temporomandibular joints provide anatomic context. Anatomic structures were derived from the CT scans and divided into finite elements to produce a mechanical FE model for this gray whale. This FE model of the gray whale is similar to the fin whale model built by Cranford and Krysl (2015). Initially, we built this gray whale model to answer one fundamental question: would it produce a similar prediction of "bone conduction hearing" as in the fin whale model from 2015? Gray whales and fin whales are members of different taxonomic Families within Mysticeti. This raised the question: are the anatomic differences between these Families extensive enough to generate a different prediction for the hearing mechanism? Subsequent model simulations predicted that gray whales also used bone conduction hearing.

The gray whale FE model was also used to design, simulate, and test experimental protocols for use in physical vibroacoustic experiments to validate the bone conduction hypothesis. The FE model was used, among other purposes, to determine how to best configure the sensors (accelerometers) on the skull by running virtual simulations with virtual sensors placed at different locations. This time-saving tool reduced the need to determine sensor placements by trial and error during the experimental phase. It is important to recognize that the FE models were not used to prove the hypothesized physiological processes involved in sound reception. The models solely provide a valuable and effective toolkit to further direct investigations of functional morphology.

It is desirable to produce FE models that use "realistic" values for tissue elasticity and density in the hope that the simulations will produce reasonable biomechanical approximations, but again the FE model should never be mistaken for what happens in actual tissue. This is why it is essential to conduct *validation* tests for all FE models (Cranford et al., 2014). Building and executing accurate models is a complex discipline in itself. At the same time, it is deceptively simple to build an *inaccurate* model with commercial software (COTS) that can lead astray, or lead in the right direction for the wrong reasons, neither of which are beneficial to the furtherance of scientific investigation and discovery.

The details of the gray whale FE model we built for this project will be published elsewhere, but those details are in some sense irrelevant here, since the model predictions were validated by the anatomic vibroacoustic experiments reported in Morris et al. (2025). The FE models we have built for this project and in previous endeavors have advanced our understanding of the underwater bioacoustic systems of whales (Cranford et al., 2008a, 2008b, 2010; Cranford et al., 2014, Cranford et al., 2015; Cranford and Krysl, 2015, Cranford and Krysl, 2018).

When we first proposed bone conduction hearing based on the results from a carefully constructed finite element model (FEM), we were met with some skepticism within the marine mammal acoustics community, with few exceptions. To date, no one has offered a plausible alternative or specific criticism, only generalized concern that our prediction may be incorrect. More to the point, skeptics suggested that the idea was "unbelievable", which may be more reflective of the novelty of the hypothesis than of any as yet undetected defects in the research itself.

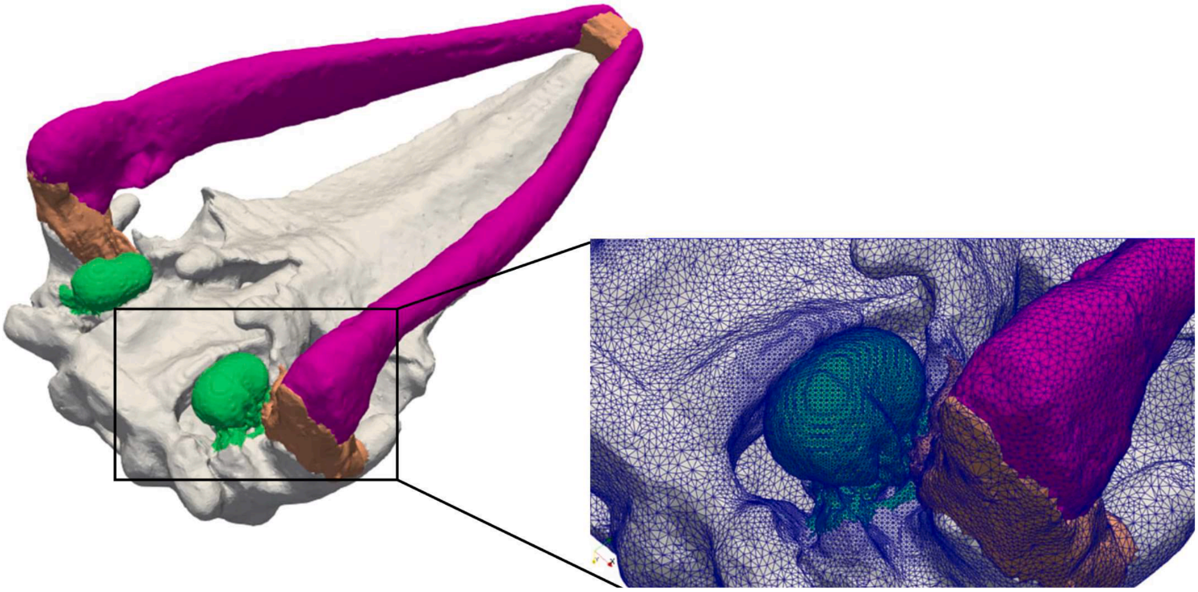

Fig. 1. Posterolateral view of the inverted gray whale skull. This figure serves two purposes; it displays the context of anatomic geometry for the auditory apparatus (skull + bilateral TPCs). The structures were reconstructed from CT scan data. Tissue types are color coded: Mandibles = magenta; TPCs = green; Cranial bones = white; TMJ (temporomandibular joint) = orange. This figure also serves as a graphical display of the mechanical finite element (FE) model constructed specifically for this study. Simply put, the model is conceptually composed of masses (nodes) interconnected by springs (elements). The inset shows the FE mesh: each "star-like" intersection represents a mass location. The interconnecting lines between masses roughly corresponds to the "springs". In this model, each vibroacoustic simulation calculates the oscillating motions for 2.5 million nodes.

We use FE models to visualize the concepts we describe. It is worthwhile to emphasize that we only use results from models to illustrate, understand or predict (simulate) experimental outcomes. Cranford and Krysl used finite element (FE) modeling to study low-frequency hearing in the fin whale (Cranford and Krysl, 2015). They found that hearing was activated by displacement and deformation of the modeled skull, referred to as the bone conduction hypothesis (see Fig. 8 in the Discussion of this paper). Building on this concept, the present study employed finite element (FE) modeling techniques to develop computational mechanical models for the gray whale skull and fin whale TPCs (Cranford and Krysl, 2015; Morris et al., 2025).

While computational FE analyses put forth the notion that the skull participates in sound reception, experimental validation was necessary, which is a large part of the work reported here. In order to validate the Bone Conduction Hypothesis (BCH) for the gray whale, we conducted a series of controlled vibroacoustic experiments. A largely denuded skull of a juvenile gray whale and its plastic replica were exposed to low frequency sounds underwater. Additional tests were conducted in air on the juvenile skull, plastic replica skull, and an adult gray whale skull. Specific bones were instrumented with accelerometers. The results consistently demonstrated amplified motions of the tympanic bullae relative to the base of the skull (Morris et al., 2025). The relative motions drive the middle ear bones to activate the inner ear. These findings provided experimental *validation* of the bone conduction mechanism as a key pathway for low-frequency sound reception in baleen whales.

For more than a century, investigators have contemplated how baleen whales might hear low-frequency sounds. Early studies suggested that low-frequency hearing in baleen whales may be driven by displacement of the skull (Lillie, 1910; Kellogg, 1928). In baleen whales, each of the bilateral tympanoperiotic complexes (TPCs) are composed of the periotic bone, two pedicles, a tympanic bulla, and a chain of three middle ear ossicles (Fig. 2). The periotic bone contains the cochlea of the inner ear. It is firmly attached and integrated into the squamosal bone of the skull base (basicranium), ensuring that the periotic bones and skull move in unison.

The mysticete TPC can be viewed as a mechanical system whose structure enables vibrations to be generated by acoustic stimuli from the ocean. As sound waves pass through the marine environment, the skull and periotic bones move in response. Vibrations of the periotic bones relative to the suspended bullae drive the fused malleus and connected ossicles, transferring energy into the cochlea.

Each tympanic bulla is suspended from the periotic/skull unit by two distinct, dissimilar pedicles, anterior and posterior (see Fig. 2). These pedicles are elongated flexible bones that allow the massive tympanic bullae to swing, or torque relative to the periotic bone and skull (Fleischer, 1980). The anatomic geometry and material properties of the pedicles and bullae determine the range, limits and complexity of the relative motions between the bulla and periotic. The malleus, first bone of each ossicular chain, is fused to the bulla. Accordingly, displacements of the bulla drive the malleus, which in turn move the incus and stapes. The footplate of the stapes transmits mechanical forces to the oval window (*fenestra ovalis*), a membrane covering the opening between the middle ear and the inner ear. At this interface, mechanical vibrations are transformed into hydrodynamic displacements within the inner ear. The bulla and ossicles function as an oscillating mass that is suspended by the spring-like pedicles to produce resonant motions with respect to the skull and periotic bone. The tympanic bulla is morphologically complex and approximately twice as dense as the other bones, with a thickened rim at the involucrum, giving it substantial inertia. Within each bony ear complex, the pedicles, bulla and ossicles constitute the *dynamic components of the TPC* (Fig. 2).

Mysticetes are sensitive to low frequency sounds (Richardson, 1995) with long wavelengths (75 m at 20 Hz, 15 m at 100 Hz). By contrast, toothed whales (Odontoceti) are primarily sensitive to high frequency sounds and possess fatty sound channels that abut their TPCs (Cranford et al., 2008b, 2010; Cranford and Krysl, 2012), with dimensions that are commensurate with the sound wavelengths at echolocation frequencies (Cranford et al., 2015). As a result, those short wavelength sounds can be effectively amplified and focused onto the surface of the TPC in odontocetes. Not so in the mysticetes. Even if fatty bodies exist (Yamato et al., 2012), their dimensions are much smaller than the long wavelengths for relevant low-frequency sounds, which can extend to multiple body lengths of these giants. As a result, it is clear that mysticete morphology lacks the requisite anatomic geometry required to focus long wavelength sounds. Because focused sound pressure is an unlikely mechanism in mysticete hearing, an alternative explanation is necessary to explain how low-frequency sounds are transmitted to the cochlea.

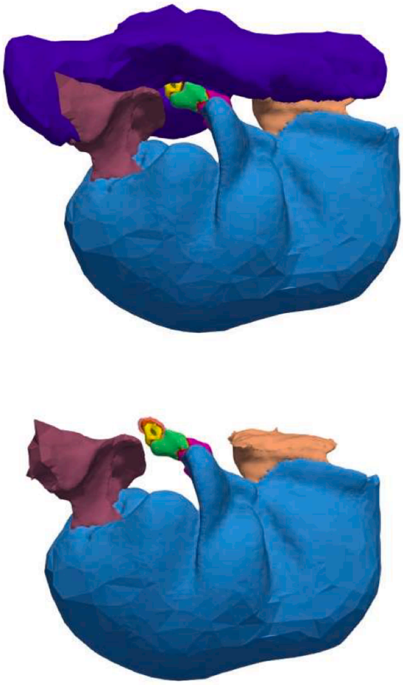

Fig. 2. Right lateral view of the bony tympanoperiotic complex from a fin whale. Upper image displays the entire TPC: Periotic = purple; Posterior pedicle = brown; Anterior pedicle = salmon; Tympanic bulla = blue; Malleus = magenta; Incus = green; Stapes = yellow. Lower image shows only the *dynamic components* of the TPC, consisting of the two pedicles, the tympanic bulla, and the middle ear ossicles. The annular ligament = orange, holds the stapes footplate in the oval window of the inner ear.

Capshaw and colleagues (Capshaw et al., 2022) conjectured that early tetrapods, despite lacking tympanic hearing, were probably sensitive to sound through bone conduction mechanisms. However, they emphasized that their use of the term “bone conduction” was non-specific; it could be used to refer to several different modes of vibration transmitted to the inner ear. They referred to the mode where the head is translated back and forth by the sound waves as the “simplest” model. This “translation of the organism” model can explain low-frequency bone conduction sensitivity in humans, and the mode of auditory stimulation for teleost fishes. How organismal translation can lead to auditory stimuli is readily explained by inertial systems, such as those for teleost otoliths (Krysl et al., 2012).

Bone conduction hearing can be interpreted to mean the process by which sound is transmitted directly to the inner ear by skull vibrations (Tonndorf, 1972), bypassing the tympanic membrane mechanism typical of mammalian systems. In contrast, Stenfelt (2013) sought to define the term "bone conducted sound" as a way in which the vibration of human skull bones could result in sound perception. Motions due to sound impulses that are transmitted through bodily tissues and involve one or more ear components (outer, middle, inner) can also produce sound perceptions. Inertial bone conduction, as proposed by Bekesy (Hood, 2005), occurs when the ossicles lag behind the vibration of the head under the influence of incident sound pressure due to their inertia. This generates relative movement between the stapes footplate and the cochlea in the same manner as for air-conducted excitation (Puria, 2020).

In mysticetes, we hypothesize that sound waves propagating through the water set the skull into motion. We also envision resonant vibrations of the bulla and ossicles (compare to skull vibration modes identified in humans (Stenfelt, 2006; Dobrev et al., 2017)). Mechanical models of the bulla, pedicles, and ossicles, in mysticetes suggest that the skull functions like the "external ear" or an acoustic "antenna" that captures sound energy and feeds it into the motion of the bulla relative to the periotic bone and skull.

The differential vibration of the TPC's dynamic components relative to the periotic bone constitutes a mechanism for transmitting sound energy into the cochlea, and is central to the bone conduction hypothesis presented here. This mechanism is enabled by the increased mass density of the highly mineralized bullae and the flexibility of the pedicles from which each bulla is suspended. It is important to note that the middle ear ossicular chain remains functional in this system. Its complex motions can be modeled using finite element analysis and visualized through dynamic simulations. These models reveal oscillating motions across various resonance modes of vibration. (See Results, Section 3.2)

2. Methods and materials

The overarching organization of this entire investigative enterprise involved multiple interdependent projects that required diverse methods, were executed over seven years, and cannot conceivably be reported in a single paper. Therefore, the details of gray whale specimen preparations for CT scanning, anatomic dissections, FE modeling, and vibroacoustic experiments will be reported separately.

Our prior anatomic work focused primarily on rorqual mysticetes, minke, fin, and humpback whales (Family: Balaenopteridae). In order to increase comparative anatomic breadth in this study, we chose to focus on the gray whale, *Eschrichtius robustus*, as an example of a non-rorqual mysticete (Family: Eschrichtiidae). The neonate gray whale specimen (LACM 97758) was obtained from the Los Angeles County Museum of Natural History. It stranded on a beach in southern California and was salvaged by the West Coast Marine Mammal Stranding Network. The intact head was removed and put into a freezer. It was subjected to CT scanning twice. After the first CT scan, much of the soft tissue superficial to the skull was removed to prepare it for vibroacoustic experiments. We refer to this as the "natural" skull because it was in superb condition when salvaged then frozen. Subsequently, we expended logistical effort to maintain the tissue in the frozen condition until it was eventually thawed for the vibroacoustic experiments.

We tested the BCH through a series of controlled underwater experiments conducted on the denuded juvenile gray whale skull. The details of those vibroacoustic experiments, procedures and results are reported in Morris et al. (2025). Here, we summarize selected findings from those experiments and present the specific results as frequency response functions that quantify the transfer of vibrational energy from the water to the motion of the bullae relative to the skull (Fig. 7). The resulting physical measurements were found to be consistent with the hypothesized bone conduction mechanism. The experimental protocols and results for the vibroacoustic experiments are fully presented in Morris et al. (2025).

The natural juvenile gray whale specimen was CT scanned twice in preparation for the physical experiments. The initial scan was conducted with all soft tissues intact. The specimen was then scanned a second time following dissection to remove most of the soft tissues superficial to the skull. This was justified by prior FEM results (Cranford and Krysl, 2015), which indicated that superficial tissues are not consequential to sound reception via the bone conduction mechanism, they could therefore be approximated as water in the FE analyses. All bony elements and ligamentous connections between the cranial bones, mandibles, periotics, pedicles, tympanic bullae, and the middle ear ossicular chains were preserved intact. In addition, a life-sized plastic replica of the skull was

Fig. 3. Ventral view of the juvenile gray whale skull reconstructed from the second set of CT scans (left) and a similar view of the 3D printed thermoplastic replica of the juvenile skull (right). (Color codes for CT scan: Skull = light blue; Mandibles = magenta; Bullae = cyan; TMJ = yellow. The scale bar pertains to the CT scan reconstruction and the artifact.).

3D-printed using ASA thermoplastic from the segmented gray whale CT scan data (Fig. 3).

Finite element (FE) models of the gray whale skull and tympanoperiotic complexes (TPCs) were developed to simulate their dynamic response to low-frequency acoustic excitation. The CT scans of the specimen were used to generate finite element meshes, with voxel values mapped to appropriate approximations of material properties for bone and ligamentous tissues.

The computational problem was formulated as a forced harmonic vibration analysis, in which incident sound waves were modeled as planar acoustic pressure fields interacting with the skull (Cranford and Krysl, 2015). The resulting dynamic loading of the TPC included both pressure-induced forces and motions imparted through vibration of the periotic bones ("bone conduction"). For each excitation frequency, steady-state vibrations were calculated, and a Transfer Function was derived to quantify the relationship between incident sound pressure and stapes velocity. Simulations also allowed visualization of complex vibrational modes of the TPC (see Results, Section 3.2).

3. Results

We examined the structural anatomy and dynamic behavior of the tympanoperiotic complex (TPC) to understand how it contributes to baleen whale hearing. The following section summarizes findings from CT scan analysis, FE modeling simulations and vibroacoustic experiments, highlighting how mechanical amplification arises within the TPC during exposure to low-frequency acoustic stimuli.

3.1. Anatomic geometry

The complex anatomic geometry within the dynamic components of the TPC (Figs. 4c & 4d) serves as the source of mechanical amplification for vibrations transmitted between the skull and bony ear complex. Both our experimental results and numerical FE simulations demonstrate that mechanical vibrations are *amplified* within the TPC. The resulting oscillating motions are ultimately transformed into hydrodynamic forces as the stapes footplate acts upon the membranous oval window and the fluids of the cochlea.

Since the periotic bone moves in concert with the squamosal bone of the skull, amplification of skull motions most likely occurs between the pedicles and the stapes footplate, as indicated by both the FE simulations and vibroacoustic measurements.

The relative motion between the bulla and the basicranium, particularly in the mediolateral axis (Fig. 7b), indicates that the bullae vibrate relative to the periotics. These relative motions initiate movement in the ossicular chain, thereby producing input to the cochlea at the stapes footplate (Cranford and Krysl, 2015).

In mysticetes, the malleus is fused to the bulla at the sigmoid process, forming a mechanical connection between the pedicles and the chain of ossicles in the middle ear (Fig. 4d). The bulla is suspended from the periotic by two pedicles, anterior and posterior (Figs. 2 & 4). The anterior pedicle has an elongate narrow attachment (4 point star) onto the “flexible” lateral wall of the bulla (4d). The posterior pedicle has a shorter, robust anchor footprint (5 point star) on the medial “inertial” wall of the tympanic bulla, close to the massive involucrum. Note that the main axis of attachment for each pedicle is approximately perpendicular to the other (Fig. 4d). These details of anatomic geometry within the dynamic components are likely consequential and significant, underscored by the complex natural modes of vibration from FE simulations. Examples are exhibited in the intricate oscillatory mechanics of the fin whale TPC that accompany the following paragraphs.

3.2. Illustrations of TPC motion

Two important (low-frequency) modes of vibration for the gray whale bullae are shown in Fig. 5, illustrated here using FE models (see simulations of modes 16▷, 18▷, 26▷, and 29▷). These modes exercise the ossicles, causing them to rock or push and pull on the stapes footplate. Note that the left and right TPCs apparently have unique acoustic “signatures”, each oscillates in different planes at different, but nearby, resonant frequencies.

It is also instructive to observe examples of intricate TPC oscillatory mechanics at resonance frequencies in the fin whale. The reader is encouraged to click through these hyperlinks to view the FEM simulations; the magnitude of displacement is color coded.

These animations are based upon the anatomic geometry, the distribution of masses and the material properties of the bones and ligaments. The Mode 1▷ animation, at 286 Hz, shows a swinging motion of the bulla and its effect on the ossicular chain. Mode 2▷, at 548 Hz, displays a slightly more complicated oscillatory pattern with a slight twist in the bulla, in addition to rocking. In both of these first two resonant frequency modes, the motion appears to be driven by the vibration of the massive tympanic bone, while the ossicles are activated in a somewhat simplistic “piston-like mode”. As resonance frequency increases, Mode 5▷ (1163 Hz) illustrates a quiescent bulla with most of the activity occurring in relatively simple oscillations of the ossicular chain. Mode 6▷ (1636 Hz) introduces motion of the sigmoid process and twisting, primarily involving the incus of the ossicular chain. Mode 10▷ (2801 Hz) demonstrates multi-planar twisting in various dynamic components of the TPC, namely the posterior pedicle, separate regions of the bulla, and the entire ossicular chain. Mode 15▷ (3985 Hz) may exhibit the most striking oscillation pattern, where the malleus appears to “lead” the rotation of the entire ossicular chain, along with flexing in the lateral wall of the bulla.

The importance of the flexible pedicles, which suspend each bulla from the periotic, is highlighted by the animated modes of vibrations above for the gray whale and fin whale. These motion pictures are crucial to fully appreciate the mechanical complexity that occurs in the bullae and ossicular chain, which cannot be completely conveyed in the text.

The range of complexity seen in these six examples of fin whale TPC oscillatory mechanics attests to the potential for encoding a plethora of acoustic parameters for transfer to the cochlea. One can easily imagine that acoustic parameters such as frequency composition, incoming trajectory, amplitude, phase, and duration could conceivably be “encoded”; is the TPC an “analog computer”? The process of transferring slightly different skull vibrations through the anatomic geometry of the TPC’s dynamic components could result in myriad unique combinations of input to the oval window.

3.3. Vibroacoustic experiments

These experiments are fully described in Morris et al. (2025). Here we provide a synopsis of experimental results for the benefit of the reader. Physical, vibroacoustic experiments were conducted with instrumented gray whale skulls underwater and in air (Fig. 6). The denuded natural skull from the juvenile gray whale and its plastic

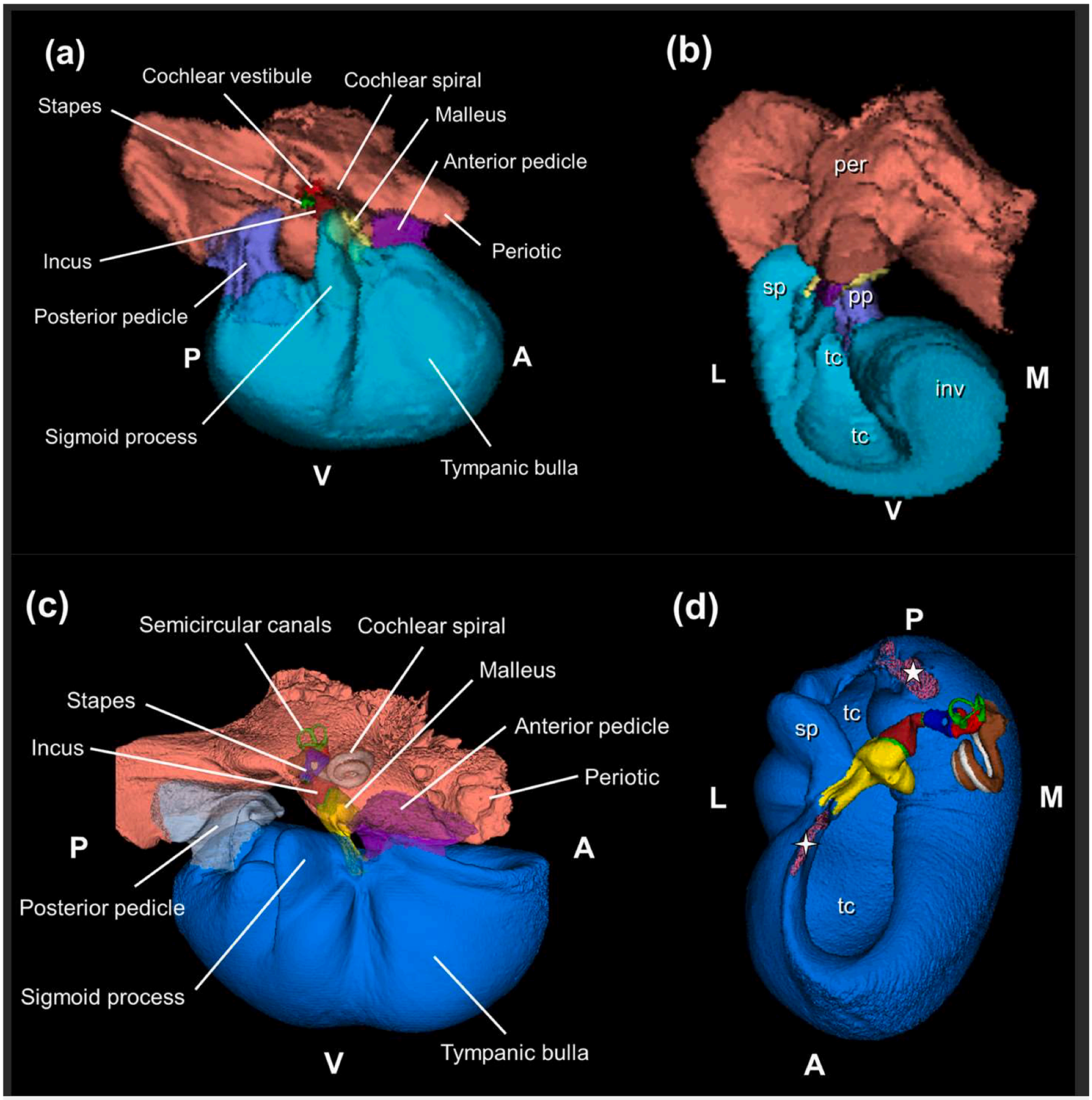

Fig. 4. Structure of the right tympanoperiotic complex (TPC) for a gray whale (4a & 4b) compared to the right TPC for a fin whale (4c & 4d), reconstructed from CT scans. The bulla is rendered in cyan for the gray whale (4a & 4b) and in blue for the fin whale (4c & 4d). (4a) shows the right lateral view of the gray whale TPC. The cochlear spiral and cochlear vestibule are components of the inner ear within the periotic bone. (4b) presents an anterodorsal view of the right TPC for the gray whale where the bulla is shown in cut-away view, demonstrating considerable disparity in thickness between the medial (M) and lateral (L) walls of the bulla. (4c) is a lateral view of the right TPC from the fin whale with landmarks labeled and transparency added to reveal internal structures. (4d) is an anterodorsal perspective of the right TPC from the fin whale. The pink attachment "footprints" (stars) show that the pedicles are fastened to the bulla on opposite sides of the tympanic cavity (tc). Observe the ossicular chain arching across the tympanic cavity, and that the stapes footplate connects to the oval window at the cochlear vestibule, the interface where the transition occurs between mechanical motion and hydrodynamic forces. Color coding of the structures in 4c & 4d are: Tympanic bulla = blue; malleus = yellow; incus = firebrick; stapes = dark blue; inter-ossicular ligaments are green; cochlear vestibule = red; semicircular canals = green; scalae of the cochlear spiral = brown and white; attachment footprints for the pedicles = pink with stars. In (4d) the cochlear vestibule, semicircular canals and scalae of the cochlear spiral are structures found within the inner ear. Abbrs. *P*=Posterior; *A*=Anterior; *V*=Ventral; *M*=Medial; *L*=Lateral; per=periotic; pp=posterior pedicle; inv=involucrum; sp=sigmoid process; tc=tympanic cavity.

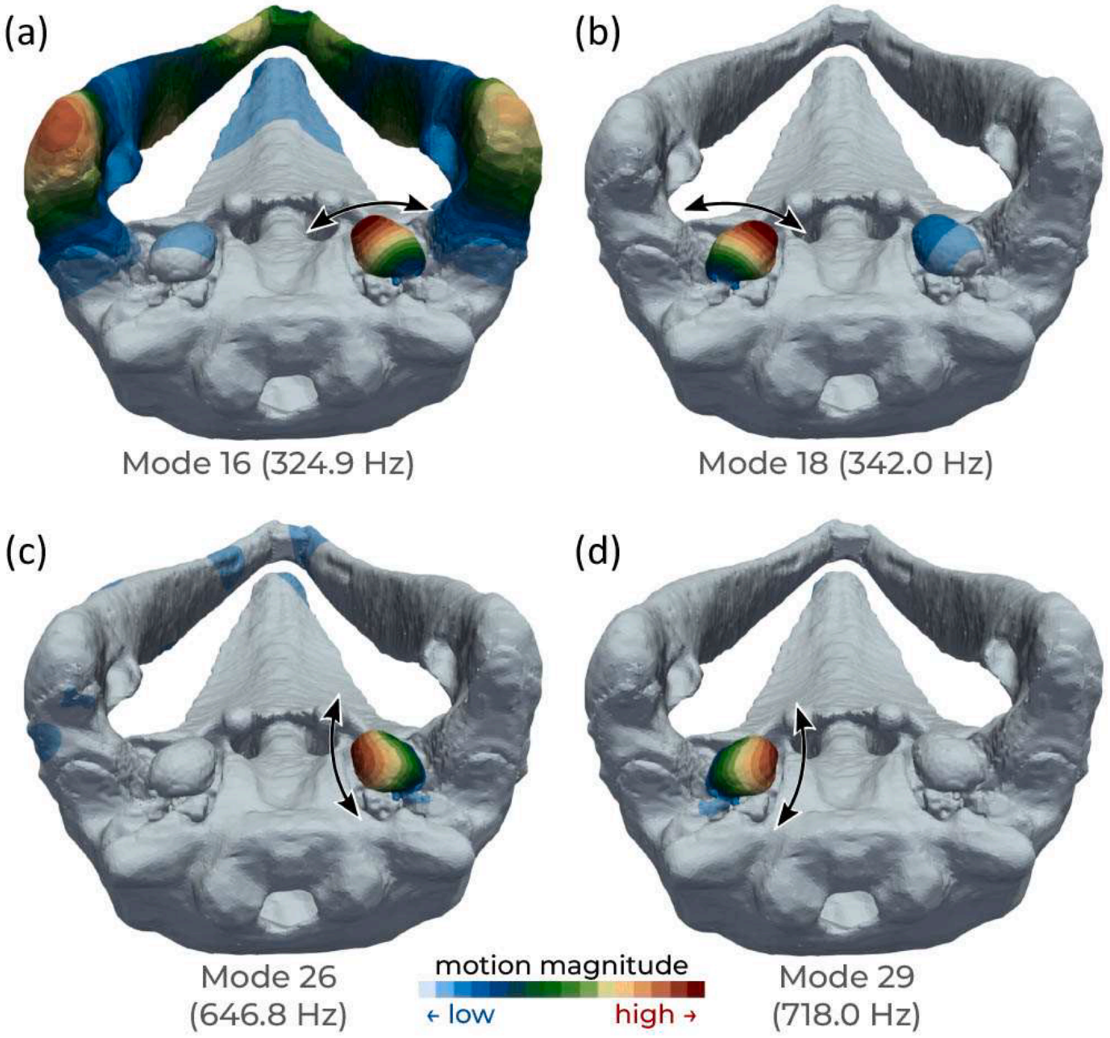

Fig. 5. Modeled modes of vibration for the tympanic bullae in the gray whale skull (a) mode 16 (324.9 Hz), (b) mode 18 (342.0 Hz), (c) mode 26 (646.8 Hz), and (d) mode 29 (718.0 Hz). The magnitude of the motion is color coded: red is high, light blue is low. The arrows indicate the directions of the rocking motion. The skull is upside down, i.e., ventral side up.

replica were tested underwater at the US Navy's transducer test and evaluation facility (TRANSDEC). The denuded juvenile skull, its plastic replica and a museum preparation of an adult gray whale skull were additionally subjected to vibroacoustic analysis in air.

The adult gray whale skull (LACM 84202) was stimulated in-air at the Los Angeles County Museum of Natural History. Vibrational excitation was applied to the base of the skull with a shaker at the foramen magnum. The juvenile and replica skulls were also tested in-air using multiple sites of stimulation, including the tip of the maxilla, the mandibular symphysis and the basicranium. These tests allow for comparisons of the measured frequency response functions between the juvenile specimen and the adult specimen: in all cases, amplified vibrations of the bullae were observed (Morris et al., 2025).

Examples of velocity response (transfer functions) for the skull base and the bullae, when excited by underwater sound arriving from the anterior direction, are shown in Fig. 7. For simple translation along the direction of the sound wave propagation, we would expect all parts of the skull to move with the same velocity. However, in Fig. 7a we see that vibration of the skull plays a role even for relatively low frequencies: the bullae experience larger velocities than the base of the skull. The interactions between the pressure waves in the water and the skull, causes the skull to oscillate. At the resonance frequencies of the bullae, these skull motions excite bullae vibrations, facilitated by their large mass and flexible attachment through the pedicles.

Fig. 7b illustrates the velocity transfer functions of the skull and bullae for the mediolateral (ML) direction (left-right axis, orthogonal to the direction of sound wave propagation). We would expect the response of the base of the skull to be relatively small, but not zero, because the skull is not perfectly symmetric, and neither is the loading by the pressure waves. Again, in the ML direction, the bullae have a significantly larger response than the skull, by about an order of magnitude (more for some frequencies than others). This means that the bullae vibrate with high amplitude relative to the skull.

This amplification can activate the ossicular chain, causing it to push, pull and torque on the stapes footplate, because in the gray whale, between 320–350 Hz (Fig. 5) the bullae pivot on the pedicles and vibrate mediolaterally (orthogonal to the direction of sound propagation). A second resonance frequency is predicted in Fig. 5, at about 700 Hz, it is associated with the bullae twisting on the pedicles. In this mode, one location on the bulla between the pedicles remains essentially

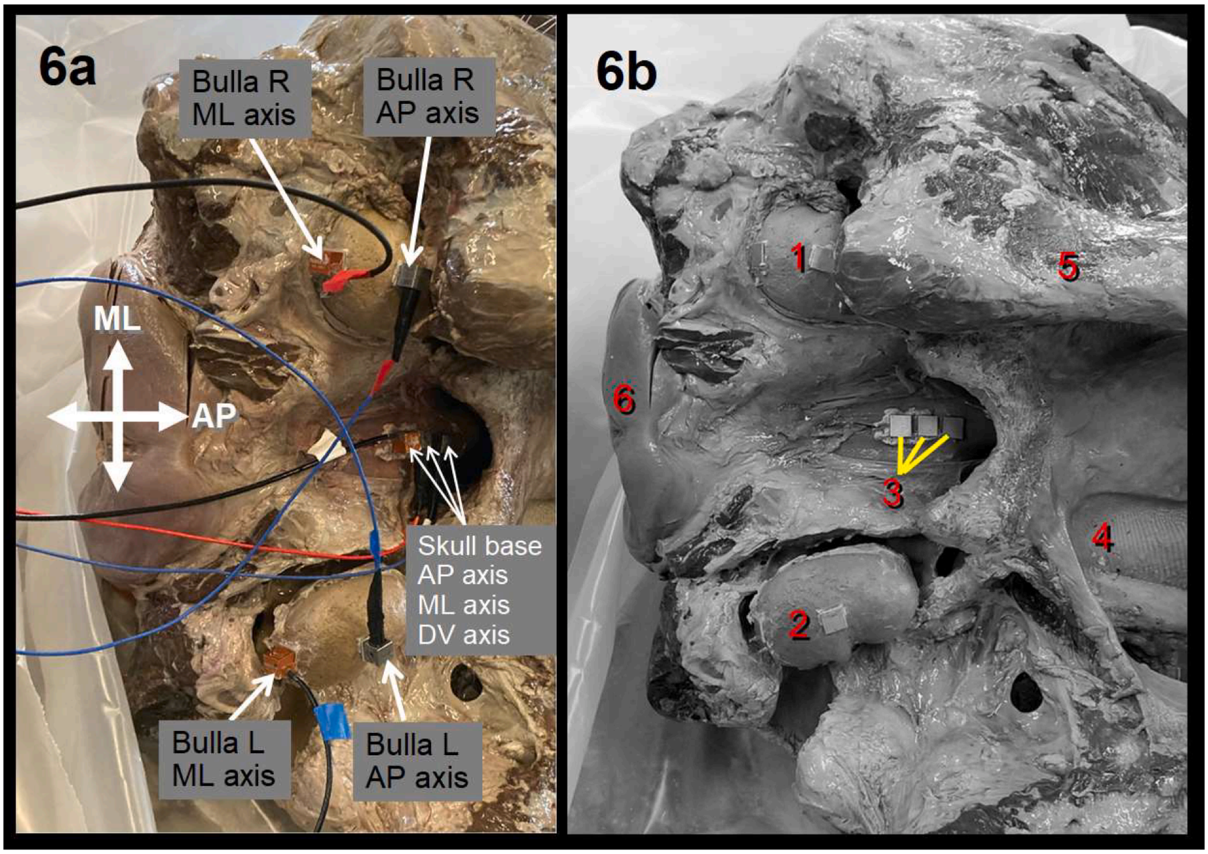

Fig. 6. Views of the ventral surface of the denuded gray whale skull instrumented for vibroacoustic recording underwater. In 6a, there are seven accelerometers depicted, three on the base of the skull and two on each tympanic bulla. Each accelerometer is oriented to measure along a specified axis: AP = anteroposterior (rostrum-tail axis), ML = mediolateral (left-right), DV = dorsoventral (back-belly axis). Figure 6b, identifies landmarks in this region of the skull and shows the square aluminum plates to which the sensors were attached: 1-Right Bulla; 2-Left Bulla; 3-Aluminum plates on basicranium. Other structural landmarks are; 4-Baleen; 5-Ramus of right mandible; 6-Occipital condyles. For details, refer to (Morris et al., 2025).

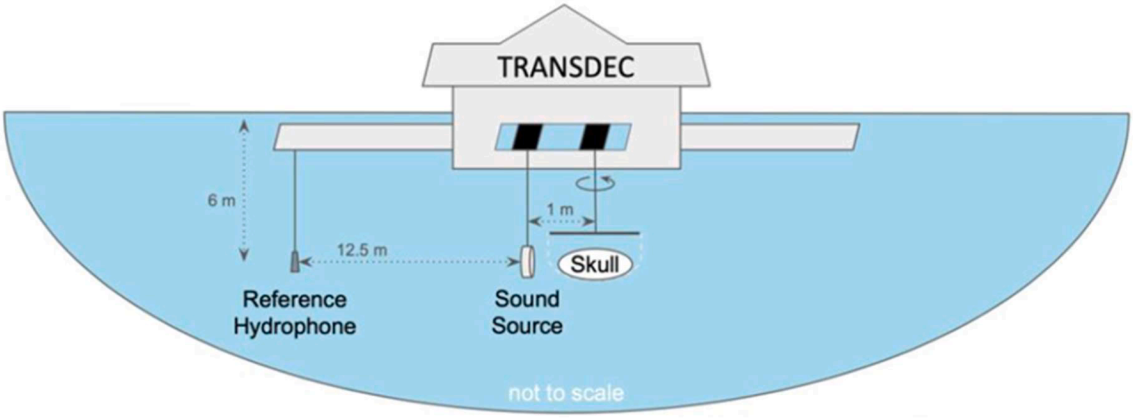

Fig. 6c. Diagram of the setup for the vibroacoustic experiments at TRANSDEC.

stationary, while anterior and posterior apexes on the bulla vibrate along the mediolateral axis. The ossicular chain is also active in these modes of vibration.

In Morris et al. (2025) the experimental results demonstrate that the replica skull exhibits resonance modes similar to those for the natural skull (Fig. 7). Although the frequency spectra are different for the natural skull and the plastic replica, likely due to differences in material properties/composition, both show significant amplification of bullae motion relative to skull motion. This suggests that the amplification is primarily due to the anatomic geometry, independent of material composition.

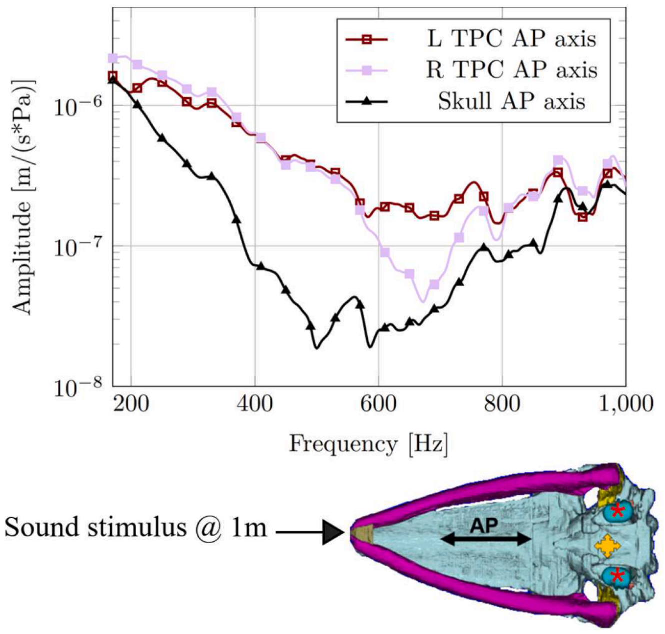

Fig. 7a. This graph represents anterior-posterior (AP) measurements from the natural juvenile skull underwater. The illustration shows the experimental configuration where the skull is ensonified by a sound source one meter away. Accelerometers are attached to the ventral keel of each bulla (red stars) and to the base of the skull (orange quad arrow). The graph shows transfer functions of velocity for each bulla compared to the base of the skull over a range of frequencies. (Experiment on 9/13/2023).

4. Discussion

The mysticete skull can be fairly characterized as a uniquely functional *external ear*, the largest of any mammal, aquatic or terrestrial. This interpretation resolves the seemingly paradoxical relationship between the long-wavelengths of low-frequency sound and relative ear “size” reported by Groves et al. (2021), as pointed out in the Introduction. Gigantic mysticete skulls apparently function as “acoustic antennas” that gather inputs for the largest ears in the world. The bullae of cetaceans also exhibit precocial development, such that they grow to adult size and shape by the time they are born or shortly thereafter (Lancaster et al., 2015).

The bone conduction system, as described here, serves as the basic hearing mechanism that receives and amplifies incoming sounds before transferring them to the cochlea in baleen whales. This bone conduction mechanism can be divided into two components: (1) low-frequency sounds from the environment interact with, and shake or displace the entire skull; and (2) the relative motion between the skull and tympanic bullae excites the dynamic components of the TPC, which mechanically amplifies these vibrations in the process of transferring them to the inner ear through the ossicular chain. As we have shown, this mechanism has been *validated* by physical vibroacoustic measurements with skulls underwater.

The FE simulations illustrate that the anatomic geometry and dynamic components within the TPC are capable of producing exceptionally complex oscillatory patterns for various resonance frequency modes. Simulations of mechanical processes for individual TPCs are based on the spatial distribution of masses (from CT scans) and the elastic properties of bony and ligamentous components.

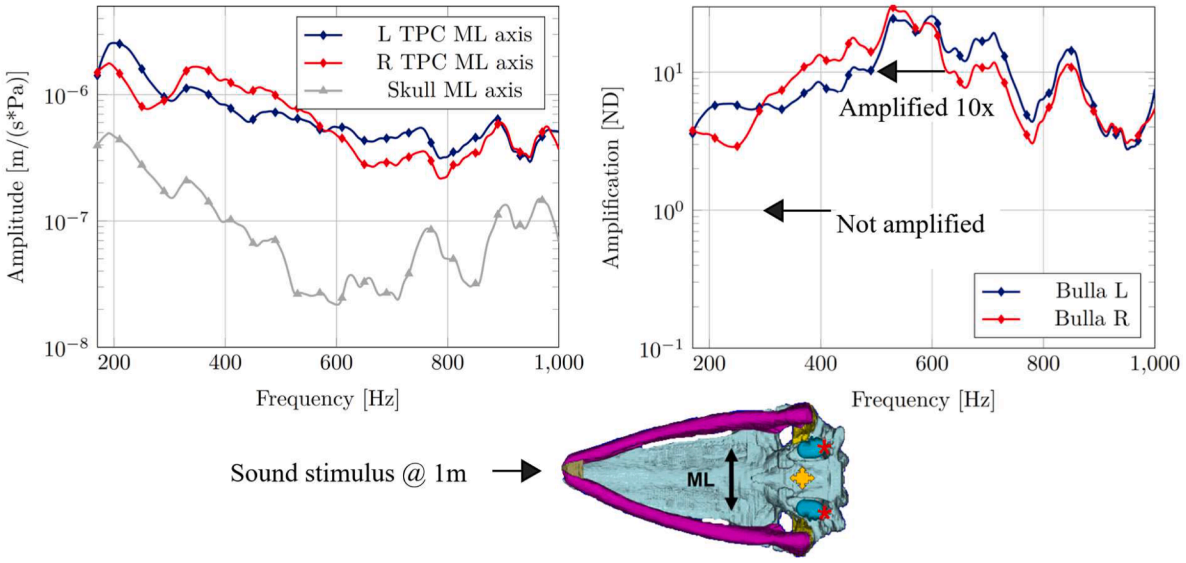

Fig. 7b. These graphs pertain to the medial-lateral measurements (L-R axis) for the natural juvenile skull underwater. The illustration shows the experimental configuration where the skull is ensonified by a sound source one meter away. Accelerometers are attached to the posterior apex of each bulla (red stars) measuring mediolateral acceleration, and to the base of the skull (orange quad arrow). The graph on the left displays the transfer functions of velocity for each bulla and base of the skull in the left-right direction (ML = mediolateral axis). The graph on the right shows the relative amplification of mediolateral velocity; the magnitude of the ML response for each bulla, divided by the magnitude of the ML response for the skull. Observe that amplification is approximately an order of magnitude, depending upon frequency. The velocity transfer function expresses how the output quantity (velocity) depends on the input (pressure loading). (Experiment 9/13/2023). See Morris et al., al.(2025) for experimental design and results.

4.1. *Acoustic forcing*

The variety of oscillatory patterns corresponding to the natural frequency modes are only part of the intricate vibration story overall. When acoustic forcing is introduced to the system, different oscillatory patterns are energized, depending upon frequency and anatomic geometry, revealing the extent of biomechanical functionality in the bone conduction mechanism.

In water, the whale's skull behaves as a floating structure. As sound waves interact with the skull, it begins to shake, it is displaced or "translated". An archetype of this phenomenon is the Rayleigh model of the motion of a sphere in an acoustic fluid (Hickling and Wang, 1966).

At very low frequencies (and therefore very long wavelengths), the skull is expected to be carried along by the progressive sound waves, almost as a rigid body. Nonetheless, this motion feeds vibrational energy into the dynamic components of the TPC (Fig. 2), which are attached to the base of the skull at the periotic bone. At higher frequencies, when the wavelengths drop below the size of the skull, the vibrations of the skull get much more complicated, responding to the complex distribution of pressure on the surface of the bones. At the intermediate frequencies, the response of the skull and the attached bones is a mixture, reflecting the continually changing acoustic environment. The vibration of the middle ear ossicles along this frequency spectrum will include a mixture of modes, depending on how effectively the acoustic impetus of the sound waves can feed energy into the nearby natural modes of vibration.

Previously, Cranford and Krysl (2015) calculated the dynamic motions and deformations of a fin whale skull due to mechanical forcing by frontal incident sound stimuli at four different frequencies. They can be inspected as dynamic illustrations of the mechanical processes in the following paragraphs. Let's envision the effects of acoustic forcing, based on FE simulations of a fin whale skull (Fig. 8).

In these four visualizations, the rigid-body translational component of the displacement in the direction of the incoming sound was *subtracted* so that the deformations of the skull stand out. To make the motions more visible, the amplitude has been magnified by 20,000 times in each of these simulations, since the actual magnitude is on the order of a small fraction of a millimeter for the assumed 180 dB excitation.

First, examine the motions for the fin whale skull subjected to 100 Hz sound waves (Fin whale skull at 100 Hz). The wavelength for 100 Hz in water is 15 m, which is about 11 times the length of this skull. Close inspection reveals that the bullae exhibit a swinging motion, which means acoustic energy is being transferred to the stapes footplate. In this case, the low frequency, long wavelength sound yields large amplitude translations or "displacements", which cause relatively minor deformation of the skull. However, as the forcing frequency increases, the translation amplitude decreases due to shorter wavelengths, as seen in this next example.

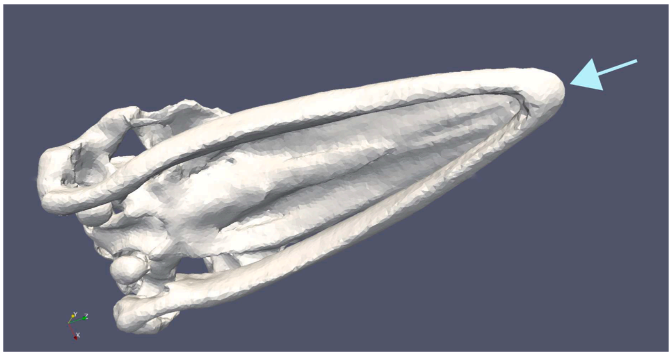

Fig. 8. This fin whale skull is 1.3 m long. In each of the linked visualizations, sound arrives from directly in front (as indicated by the arrow), only the frequency of the sound stimulus changes in each case. The reader is encouraged to execute each hyperlink to examine the calculated motions and deformation responses of the fin whale skull at four different resonant frequencies.

Now examine the skull motions calculated for 250 Hz incident sound waves (Fin whale skull at 250 Hz). At this frequency, the wavelength in water is 6 m, approximately 4.5 times the length of this skull. The higher forcing frequency results in reduced amplitude of skull translation, but increases the complexity of deformation or warping. The increased motion of the tympanic bullae is also perceptible. That is partially due to the amplification mechanism within the dynamic components of the TPC.

Fin whale skull motions computed for 1 kHz incident frontal sound waves are shown next (Fin whale skull at 1 kHz). At this frequency, the wavelength in water is 1.5 m, nearly equal to skull length. Now the skull responds in complicated ways, more complex deformation, as forcing wavelength begins to approximate skull size. Also, note that the bullae are beginning to twist as well as rock.

Finally, fin whale skull motions for 2 kHz incident sound waves are visualized (Fin whale skull at 2 kHz). At this frequency, the wavelength is 0.75 meter in water, approximately half of the skull's length. Once the forcing frequency is sufficiently high, and the wavelength is some fraction of skull length, the skull tends *not* to translate as a whole. Instead, it exhibits an intricate and complex response due to its interactions with smaller wavelengths. The trend is toward complex patterns of warping and twisting, as seen in the bullae. These four examples illustrate the essence of the bone conduction mechanism as we currently understand it.

4.2. *Implications from bone conduction hearing in mysticetes*

Implications that can be drawn from bone conduction hearing and the amplification mechanism within the TPC are significant for understanding mysticete natural history. Based on our multi-species simulations, anatomic comparisons and vibroacoustic measurements, it appears that the bone conduction mechanism incorporates the skull to function in a manner similar to the "external" or outer ear of terrestrial mammals or the seismic sense in other vertebrates (Narins and Lewis, 1984; Cranford and Krysl, 2015, Cranford and Krysl, 2018; Morris et al., 2023, 2025).

The mysticete skull appears to function as an "acoustic antenna", gathering various acoustic inputs and processing the resulting bony vibrations through the TPC as mechanical motions. Evidently, these vibrations contain information about acoustic trajectory, frequency composition, duration, bandwidth, intensity or loudness and phase, inevitably transferring these parameters as input(s) to the cochlea of the inner ear.

The bone conduction mechanism undoubtedly enables mysticetes to be sensitive to long-wavelength low-frequency sounds underwater across vast open ocean distances (Payne and Webb, 1971; Payne, 1995; Clark and Ellison, 2004; Širović et al., 2007; Zhu and Wen, 2024). Roger Payne should be credited as the first to explore the logical ramifications and implications of mysticete long-range acoustics (Payne and Webb, 1971; Payne, 1995). At that time, precious little was known about baleen whale hearing, particularly in relation to LF acoustic signals being sent and received underwater across immense distances. Payne's propositions were ahead of their time. It is remarkable that his suppositions are not more widely recognized or cited today, despite his insightfully reasoned and exquisitely constructed arguments (Payne, 1995; Tyack, 2022).

"To summarize the evidence currently in support of the theory of long-range communication: … Mating is known to be at a minimum during the one time of year when fin whales are most concentrated, and at a maximum during the time when they are thinly dispersed over millions of square miles of ocean. There are no known breeding concentrations for fin whales. Krill are notorious for appearing in unpredictable locations far from regions of previous high concentration, yet wherever krill form their concentrations in different years, fin whales assemble to feast on them. The overall picture of fin whale migrations is one of apparently disorderly movements in which the whales don't follow definite rules. The many exceptions to the stereotyped rules of migration show that fin whales are apparently able to come together at will, even during seasons when they are known to be broadly spread over the ocean. There are also reports of occasional large concentrations of fin whales in areas in which they are usually only sparsely distributed. All these otherwise inexplicable observations would be explained by fin whales possessing a means of signaling to each other over long distances" Payne (1995) (p. 187).

According to Payne, a fin whale "heard" may be the largest group of acoustically connected individuals spread across the greatest distance for any marine mammal species. Dependence upon low-frequency sensitivity within the auditory apparatus, along with the neurological capacity to extract signals from noise, determine the operational range, which could stretch to hundreds or thousands of square kilometers. It is admittedly difficult to fathom such a notion, but it is unreasonable to argue against it considering the current state of our knowledge regarding mysticete natural history (Tyack, 1997; Clark and Gagnon, 2002; Watkins et al., 2004; Širović et al., 2007; Brownell et al., 2008; Frasier et al., 2011; Širović and Hildebrand, 2011; Širović et al., 2013; Weirathmueller et al., 2013; Davis et al., 2020; Herr et al., 2022; Soldevilla et al., 2022b, 2024).

Low-frequency (LF) hearing in mysticetes likely influences many aspects of their natural history. The acoustic sensory system is undoubtedly critical to their survival, conceivably providing navigational information regarding environmental features like continental shelf escarpments, islands, sea mounts or ridges, perhaps current systems, hydrothermal vents, upwelling, or large dense food patches by low-frequency sound navigation and ranging (Clark and Ellison, 2004).

The mysticete acoustic sense likely promotes inordinately long distance "communication" perhaps aided by the SOFAR channel (Ewing and Worzel, 1948; Webb and Tucker, 1970), yielding information on the boundaries and dispersal patterns of social entities and/or arousal states of conspecifics for feeding or mating (Payne, 1995; Herr et al., 2022).

4.3. *Energetics of long-distance signaling*

It has long been known that some mysticete sounds are monotonous and repetitive, often produced constantly for days or weeks on end, all while traveling great distances (Winn and Perkins, 1976; Clark and Gagnon, 2002; Clark and Ellison, 2004; Watkins et al., 2004; Širović et al., 2007; Soldevilla et al., 2022b). This raises two questions: (1) What is the energetic cost of this constant soniferous behavior? (2) What are its functions? Despite the high intensity of baleen whale sounds (~189 dB re 1 μPa at 1 m (Širović et al., 2007; Weirathmueller et al., 2013), they are thought to be energetically *inexpensive*.

"It is easy to be impressed by how loud the sounds of the fin whale are and how far they travel. But the surprising thing is not that they are loud but that sounds of such relatively little energy should be audible so far away in the sea. The fact that they propagate for long distances is a consequence of the strange characteristics of ocean acoustics. And the fact that they are still audible after such long journeys is a consequence of the exquisite sensitivity of the vertebrate ear." (Payne, 1995, page 188), (Also see Payne, 1995, page 359, Appendix: A Primer of Ocean Acoustics).

"As loud as fin and blue whale sounds are, the power in their blips is really only about ten acoustic Watts—about the same power as the light that radiates from a thirty-watt fluorescent bulb" (Payne, 1995).

Given this, it is reasonable to suggest that the superb LF sensitivity provided by bone conduction hearing may have increased selective pressure to produce higher amplitude sounds over time in order to increase sensory and social reach. In particular, these "acoustic" selective pressures could reasonably spawn "cooperation" in finding and exploiting concentrated patches of food spread across wide expanses of ocean. This appears to be a viable strategy for some mysticetes, like bubble nets in humpbacks and lunge feeding fin whales (Sharpe, 2001; Wiley et al., 2011; Herr et al., 2022; Cade et al., 2023; Szabo et al., 2024). Large rorqual feeding aggregations are well known. Are they attracted by incidental production of feeding sounds or purposeful communication of bonanzas (Brodie, 1993; Tyack, 1997; Stimpert et al., 2015)?

4.4. *Communication*

In the open ocean, minimal attenuation characteristics for low frequency sound promotes long distance communication. Some types of mysticete sounds have often been characterized as universally repetitive and monotonous, but that does not hold for all categories of their sounds. The complex "songs" of multiple mysticete species, like bowhead or humpback whales, are relatively short in duration (minutes), often objectively and beautifully melodic to the human ear, constantly changing and ascribed to multiple functions and social "displays" (Payne and Webb, 1971; Payne and McVay, 1971; Tyack, 1981; Dahlheim et al., 1984; Payne and Payne, 1985; Tyack, 1997; Clark and Gagnon, 2002; Darling et al., 2006; Delarue et al., 2009; Tervo et al., 2011; Darling et al., 2012, 2014; Stimpert et al., 2015; Tyack, 2022). Most mysticetes produce a variety of sounds (Norris et al., 1977; Thompson et al., 1979; Watkins, 1981; McDonald et al., 1995; Edds-Walton, 1997; Gedamke et al., 2001; Clark and Gagnon, 2002; Parks et al., 2005; McDonald et al., 2006; Širović et al., 2007; Brownell et al., 2008; Tervo et al., 2009; Širović et al., 2014; Varga et al., 2018; Davis et al., 2020; Soldevilla et al., 2022a, 2022b; Helble et al., 2024; Soldevilla et al., 2024). Likewise, the complexity of motion in the TPC that we observe in simulations of the bone conduction mechanism could be useful to whales in discriminating between the various songs and sounds.

4.5. *Predator avoidance*

The low frequency bandwidth given by the mechanisms of bone conduction hearing and amplification affords some mysticetes the ability to eavesdrop on their predators (Cummings and Thompson, 1971; Frankel and Stein, 2020). Killer whales (*Orcinus orca*) are the only known predator on baleen whales, most commonly preying upon gray and minke whales. Branstetter and colleagues (Branstetter et al., 2017), found the low-frequency hearing cutoff (>100 dB re μPa) for killer whales at 600 Hz, indicating that gray and minke whale vocalizations should be well within the audible range of *Orcinus* sp. Conversely, large balaenopterids and balaenids tend to produce repetitive sounds below the low frequency cutoff for killer whales, opening a potentially rich channel for surreptitious communications beyond earshot of these predators.

4.6. *Collision avoidance*

The momentum carried by a large swimming mysticete, that may weigh more than 100 metric tons (Nishiwaki, 1950; Tomilin, 1967; Lockyer, 1976), suggests that a collision could potentially be catastrophic. The acoustic sensory system is the most likely modality to provide infallible information regarding the locations of other large whales or objects in the environment, in order to avoid dangerous kinetic collisions. Payne (1995) thought collision avoidance was an important consideration because of the enormous forces involved if a collision were to occur at any common swimming speed, particularly when the ocean is often dark and murky or may be full of prey at high densities.

It is striking that intervals between acoustic pulses (IPIs) are often so brief (<1 s.) and repetitious when mysticetes are in close proximity, as reported by multiple authors (Stimpert et al., 2007; Herr et al., 2022; Soldevilla et al., 2022b; Zhu and Wen, 2024). Could these pulses be used to avoid bumping into one another, by transmitting "simple signaling of place" (Payne and Webb, 1971; page 110)? Perhaps pulsed sounds with short IPIs help to make conspecifics aware of others in close proximity in order to avoid collisions. Otherwise, what would be the point of making sounds so rapidly and often in the open ocean? These rapid repetition rates seem reminiscent of echolocation pulse rates, but the behavior of baleen whales in most reported instances do not suggest echolocation as a pertinent explanation. The point here is that all or most of these essential functions are mediated by bone conduction hearing in mysticetes, i.e., the acoustic sensory system is essential to their survival (Nowacek et al., 2004, 2007; McKenna et al., 2015; Herr et al., 2022; Tyack, 2022).

4.7. Evidence for what whales can hear

Conducting direct hearing tests with animals the size of mysticetes is a significant challenge and, thus far, have been marginally productive (Kleivane et al., 2024). As a result, our understanding of what and how well mysticetes hear, are relegated to rather coarse measures based upon their responses to acoustic exposure of various designs (Cummings and Thompson, 1971; Dahlheim, 1983; Tyack, 1983; Mobley et al., 1988; Frankel and Clark, 1998; Nowacek et al., 2004, 2007; Southall et al., 2009; Tyack et al., 2011; Dahlheim and Castellote, 2016; Sivle et al., 2016; Southall et al., 2016; Kvadsheim et al., 2017; Dunlop, 2018; Erbe et al., 2019; Frankel and Stein, 2020; Thode et al., 2020; Southall et al., 2023).

Computational (FE) modeling (when validated), along with anatomic studies, provides valuable and detailed bioacoustic predictive capabilities. For example, FE modeling can be used to predict frequency sensitivity by constructing computational audiograms (Cranford and Krysl, 2015), and directional hearing maps or head-related-transfer-function (HRTF) (Krysl and Cranford, 2016; Cranford and Krysl, 2018).

Perhaps the most powerful FE tools are those that offer the capacity to conduct "virtual experiments". These tools allow us to manipulate features within the finite element models and then observe the effects in subsequent simulations, valuable tools for functional analysis. The FE computational platform also makes it possible to simulate extreme acoustic conditions, to which it would be unethical to expose live animals.

4.8. There is much we do not know

How well can mysticetes pick a signal out of noise? The amplification mechanism we described in the TPC probably helps in this regard. The brains of mammals are large relative to other vertebrates. Whale brains are among the largest in existence. Mysticetes have hypertrophied auditory centers and tracts within the brain, not to the same degree as in odontocetes but more highly developed than in most mammals (Breathnach, 1960; Ridgway, 2000).

We should not discount the possibility that a bone conduction mechanism for LF hearing may also be operational in all or some odontocetes, particularly those with solid bony connections between the skull and the bullae (i.e., sperm whales and beaked whales). Some evidence for that possibility already exists (Krysl et al., 2006; Cranford et al., 2010, Cranford et al., 2015; Escobar, 2016).

Equally intriguing is the idea of directional hearing, but that topic is beyond the scope of this paper and would require a dedicated research effort to investigate adequately. We assume that mysticete directional hearing is a near certainty, because otherwise there would be limited value in hearing a sound for which the source location is unknowable. In previous work, we found preliminary evidence for directional hearing in mysticetes (Cranford and Krysl, 2018).

5. Conclusions

In the present study, we have demonstrated that relative motion between the periotic bone (rigidly integrated into the base of the mysticete skull) and the dynamic components of the tympanoperiotic complex (TPC) – including the pedicles, tympanic bullae, and ossicular chains – serve as a key mechanism for amplifying and transmitting sound energy from the marine environment to the cochlea of the gray whale. The anatomic geometry of these dynamic, interconnected components governs both the complexity and amplitude of vibrational motion in response to low-frequency stimuli. These mechanical motions, are ultimately presented to the cochlea via input from the stapes footplate.

The hypothesis that the skull plays a significant role in mysticete hearing, first proposed by Cranford and Krysl, (2015), was based on the results of FE simulations conducted with a fin whale model. Here we have used physical experiments to validate the bone conduction hypothesis. The mechanism described here can be broadly termed bone conduction; however, it is important to emphasize that the processes observed in mysticetes differ fundamentally from conventional bone conduction mechanisms in humans (e.g., Tonndorf, 1972; Stenfelt, 2013; Hood, 2005; Puria, 2020).

The bone conduction mechanism is likely functional in all mysticetes due to commonalities of anatomic geometry and functional morphology.

We tested the bone conduction mechanism using vibrational analysis performed on the skulls of gray whales (Morris et al., 2025). Sounds were projected underwater toward skulls instrumented with accelerometers on the base of the skull and the tympanic bullae (Figs. 6 & 7). The frequency response functions (Fig. 7) demonstrate that skull vibrations, due to interactions with underwater sound, result in amplified differential motion of the bullae relative to the skull (Figs. 7 & 8). These relative motions excite the ossicular chain and transmit stimuli to the inner ear.

The mysticete auditory system is a specialized evolutionary adaptation for low-frequency underwater hearing, distinct in both scale and biomechanical function.

In subsequent publications we will proceed to *validate* the finite element models using the skull measurements collected in the physical experiments (Morris et al., 2025). Validation of the finite element models will bolster confidence in a variety of computational investigations going forward. Future planned studies of primary importance include comparisons of sound reception mechanisms for multiple mysticetes, starting with the gray whale, the fin whale and the minke whale. Additionally, we intend to create intriguing predictions for specific functions of the hearing apparatus, including computational audiograms (Cranford and Krysl, 2015) and head-related-transfer function (HRTF) beginning with the gray whale (both studies are currently underway).

Dedication

As first author and as a point of personal privilege, I would like to dedicate this paper to a few of my most influential mentors: Kenneth S. Norris, A. Todd Newberry, Paul Nachtigall, Sam H. Ridgway, James G. Mead, Dominique Homberger, Søren Hechmann Andersen, R. Ewan Fordyce, John M. Olguin and "the Carls" Carl E. Rischer and Carl R. Schilt. Each of them sparked my enthusiasm for scientific curiosity and sculpted my penchant to forge ahead despite warnings about many supposed "impossible" projects; like the *seven year saga* reported here. I am deeply indebted to them all.

Funding

When we first reported the prediction of bone conduction hearing in mysticetes, there was skepticism from within the marine mammal acoustics community. Fortunately, Dr. Michael Weise (Office of Naval Research) stepped forward to take a chance that we might be correct, perhaps because we had successfully completed other projects that had been deemed “impossible”. Dr. Weise funded the preliminary study in 2018 that successfully tested our methods of skull preparation. In 2019, the Subcommittee on Ocean Science and Technology (SOST) selected our study to pursue and eventually produce the validation evidence for mysticete bone conduction hearing. This work was funded by the SOST consortium of federal agencies: we appreciate the stalwart support from Dr. Michael Weise, Program Manager and Dr. Sarah Weiss, Marine Mammals and Biological Oceanography Program, Office of Naval Research; Dr. Erica Staaterman, Center for Marine Acoustics, Bureau of Energy Management; Anu Kumar and Mandy Shoemaker, Living Marine Resources Program, Naval Facilities Engineering and Expeditionary Warfare Center (NAVFAC EXWC).

Office of Naval Research (ONR) Award number: N00014–19–1–2682 (TC, PK, JH).

Office of Naval Research (ONR) Award number: N00014–18–1–2797 (TC, PK).

CRediT authorship contribution statement

Ted W. Cranford: Writing – review & editing, Writing – original draft, Visualization, Validation, Supervision, Software, Resources, Project administration, Methodology, Investigation, Funding acquisition, Formal analysis, Data curation, Conceptualization. **Margaret A. Morris:** Writing – review & editing, Writing – original draft, Visualization, Validation, Supervision, Software, Project administration, Methodology, Investigation, Formal analysis, Data curation. **Petr Krysl:** Writing – review & editing, Writing – original draft, Visualization, Validation, Supervision, Software, Resources, Project administration, Methodology, Investigation, Funding acquisition, Formal analysis, Data curation, Conceptualization. **John A. Hildebrand:** Writing – review & editing, Writing – original draft, Visualization, Validation, Supervision, Resources, Project administration, Methodology, Investigation, Funding acquisition, Formal analysis, Conceptualization.

Declaration of competing interests

Authors have no competing interests to declare.

Acknowledgements

Working with giant whales always requires many helping hands. Special appreciation goes to Dr. Martin Jones at Ford Motor Company. He provided access to the Nondestructive Evaluation Laboratory, as well as the time, expertise, and resources to CT scan the neonate gray whale head on two separate occasions. We greatly appreciate all those who helped us prepare and conduct the experiments at the US Navy Transducer Evaluation Center: Steve Pucillo, Jennifer Jeffress, Beverly Kennedy, Greg Montoya, Simone Baumann-Pickering, Bruce Thayer, Kieran Lenssen, Kaya Cohen, Ian Cosgrove, Katrina Johnson, Ben Stivi, Isabelle Jeuris, Hadley Clark, Lauren Baggett, Gabrielle Arrieta, Morgan Ziegenhorn, Isabel Catalina Barrera Diaz, Tean Brooks, Vanessa Zobell, Macey Rafter, Eric Snyder, Rebecca Cohen, Ally Rice, Alejandro Cano-Lasso Carretero and Sean Wiggins.

Construction of specialized equipment was accomplished with the time and expertise of: Vince Crivello, a fisherman and expert in net construction who built the monofilament net-bag and hanger designed to hold the submerged skulls in the test tanks. We also appreciate Michael Scott and Dan Fuller (Inter-American Tropical Tuna Commission) who identified Vince Crivello. Many thanks to John Joseph of Shoot-A-Way, Inc. who provided the large mesh monofilament net material used to construct the net-bag that held the skulls at TRANSDEC. Customized specimen transporters were constructed by Lionel Naraidu, USAF; Genaro Franco USMC Ret.; Shane Fredericks, USMC; and Jeff Graw, USN Ret.

Essential invaluable expertise during processing and multiple dissections of the gray whale specimen was provided by: Dr. Winston Lancaster, University of Alabama at Birmingham; Dr. Joy Reidenberg, Mt. Sinai School of Medicine; Dr. Erin Paig-Tran, California State University, Fullerton and her entire necropsy crew; Dr. Alissa Demming, Pacific Marine Mammal Center with their fabulous extrication vehicle. Kerri Danil, Kathryn Sherman and Elyse Wurster at NOAA Federal provided assistance and access to facilities at the Southwest Fisheries Science Center to complete denuding of the skull, with help from Lexi Mena, Jessica Ruth, Alaina Harmon, Rory Driskell and Matt Carriveau. Other essential contributors were: Dr. Wesley Elsberry (signal processing), Mark Todd (computer construction, maintenance and repair), Murray Foster (3D printing) and Jennifer Jeffress. We also thank Carol Fairfield along with the other Alaska humpback whale helpers Sasha Ertl, Sheyna Wisdom, and Colleen Shannon, as well as Dr. Barbara A. Mohoney, Protected Resources Division NMFS. Long Marine Laboratory, UC Santa Cruz provided access to comparative mysticete specimens and expertise from Dave Casper, DVM, Megan Moriarty, DVM, Robin Dunkin, PhD and Maria Choy. We greatly appreciate John Ososky, Charles Potter, and Dr. James Mead at the National Museum of Natural History (Smithsonian) for specimen loans and expert advice. Dr. John Reiss at California State Polytechnic University, Humboldt, provided access to a prepared minke whale skull and expert analysis with discussions of osteological anatomic geometry between the skull base and TPCs.

We appreciate the help, observations and expertise provided by Flip Nicklin and Dr. Bruce Mate, as well as the long term support and editorial prowess of Dr. Bob Gisiner. Dr. Mats Amundin continues to provide innovative ideas and sage council.

We thank the Los Angeles County Museum of Natural History (LACM), especially Dr. Jorge Velez-Juarbe and Dave Janiger for providing the primary gray whale specimens used in this study. We appreciate those who assisted with in-air vibroacoustic experiments on the adult gray whale skull at the museum, Nina Folz and Shannon Dolan. Eric Anthony, assisted by Dr. Winston Lancaster, produced exquisite photographs of the skulls and osteological procedures at LACM.

The Pacific Marine Mammal Center and the Natural History Museum of Los Angeles County were valuable contributors to this work by collecting and preserving the pristine gray whale specimen used in this study. Both are members of the West Coast Marine Mammal Stranding Network. We greatly appreciate their valiant efforts on our behalf.

The manuscript was improved by feedback from multiple anonymous reviewers.

Data availability

Data will be made available on request.

References

Branstetter, B.K., Leger, J.S., Acton, D., Stewart, J., Houser, D., Finneran, J.J., Jenkins, K., 2017. Killer whale (*Orcinus orca*) behavioral audiograms. J. Acoust. Soc. Am. 141, 2387–2398.

Breathnach, A.S., 1960. The cetacean central nervous system. Biol. Rev. 35, 187–230.

Brodie, P.F., 1993. Noise generated by the jaw actions of feeding fin whales. Can. J. Zool. 71, 2546–2550.

Brownell, R.L.J., Nowacek, D.P., Ralls, K., 2008. Hunting cetaceans with sound: a worldwide review. J. Cetacean Resour. Manag. 10, 81–88.

Cade, D.E., Kahane-Rapport, S.R., Gough, W.T., Bierlich, K.C., Linsky, J.M.J., Calambokidis, J., Johnston, D.W., Goldbogen, J.A., Friedlaender, A.S., 2023. Minke whale feeding rate limitations suggest constraints on the minimum body size for engulfment filtration feeding. Nat. Ecol. Evol. 7, 535–546.

Capshaw, G., Christensen-Dalsgaard, J., Carr, C.E., 2022. Hearing without a tympanic ear. J. Exp. Biol. 225.

Clark, C.W., Ellison, W.T., 2004. Potential use of low-frequency sounds by baleen whales for probing the environment: evidence from models and empirical measurements. In: Thomas, J.A., Moss, C.F., Vater, M. (Eds.), Echolocation in Bats and Dolphins. The University of Chicago Press, Chicago, pp. 564–589.

Clark, C., Gagnon, G., 2002. Low-frequency vocal behaviors of baleen whales in the North Atlantic: insights from Integrated Undersea Surveillance System detections, localization, and tracing from 1992 to 1997. US Navy J. Underwater Acoust. 52, 609–640.

Cranford, T.W., Amundin, M., Krysl, P., 2015. Sound production and sound reception in delphinoids. In: Herzing, D.L., Johnson, C.M. (Eds.), Dolphin Communication and Cognition: Past, Present, and Future. MIT Press, Cambridge, pp. 19–48.

Cranford, T.W., Krysl, P., 2012. Acoustic function in the peripheral auditory system of Cuvier's Beaked Whale (*Ziphius cavirostris*). In: Popper, A.N., Hawkins, A.D. (Eds.), Effects of Noise on Aquatic Life. Springer Science+Business Media, LLC, New York, pp. 69–72.

Cranford, T.W., Krysl, P., 2015. Fin whale sound reception mechanisms: skull vibration enables low-frequency hearing. PLoS ONE 10, e116222.

Cranford, T.W., Krysl, P., 2018. Sound Paths, Cetaceans. In: Würsig, B., Thewissen, J.G.M., Kovacs, K. (Eds.), Encyclopedia of Marine Mammals. Academic Press/Elsevier, San Diego, pp. 963–966.

Cranford, T.W., Krysl, P., Amundin, M., 2010. A new acoustic portal into the odontocete ear and vibrational analysis of the tympanoperiotic complex. *PLoS One* (Public Lib. Sci.), e.0011927.

Cranford, T.W., Krysl, P., Hildebrand, J.A., 2008a. Acoustic pathways revealed: simulated sound transmission and reception in Cuvier's beaked whale (*Ziphius cavirostris*),. Bioinspir. Biomim. 3, e016001.

Cranford, T.W., McKenna, M.F., Soldevilla, M.S., Wiggins, S.M., Shadwick, R.E., Goldbogen, J., Krysl, P., St Leger, J.A., Hildebrand, J.A, 2008b. Anatomic geometry of sound transmission and reception in Cuvier's beaked whale (*Ziphius cavirostris*)," Anat. Rec. 291, 353–378.

Cranford, T.W., Trijoulet, V., Smith, C.R., Krysl, P., 2014. Validation of a vibroacoustic finite element model using bottlenose dolphin simulations: the dolphin biosonar beam is focused in stages. Bioacoustics 23, 161–194.

Cummings, W.C., Thompson, P.O., 1971. Gray whales, Eschrichtius robustus, avoid the underwater sounds of killer whales, *Orcinus orca*. Fishery Bull. 69, 525–530.

Dahlheim, M., Castellote, M., 2016. Changes in the acoustic behavior of gray whales *Eschrichtius robustus* in response to noise. Endanger. Species Res. 31, 227–242.

Dahlheim, M.E., 1983. Responses of Gray Whales (*Eschrichtius robustus*) to Nonbiological Noise. J. Acoust. Soc. Am. (Suppl 74).

Dahlheim, M.E., Fisher, H.D., Schempp, J.D., 1984. Sound production by the gray whale and ambient noise levels in Laguna San Ignacio, Baja California Sur. In: Jones, M.L., Swartz, S.L., Leatherwood, S. (Eds.), The Gray Whale. Academic Press, Inc, MexicoNew York, pp. 511–541.

Darling, J.D., Acebes, J.M., Yamaguchi, M., 2014. Similarity yet a range of difference between humpback whale songs recorded in Philippines, Japan and Hawaii in 2006. Aquat. Biol. 21, 93–107.

Darling, J.D., Jones, M.E., Nicklin, C.P., 2006. Humpback whale songs: do they organize males during the breeding season? Behaviour 143, 1051–1101.

Darling, J.D., Jones, M.E., Nicklin, C.P., 2012. Humpback whale (*Megaptera novaeangliae*) singers in Hawaii are attracted to playback of similar song. J. Acoust. Soc. Am. 132, 2955–2958.

Davis, G.E., Baumgartner, M.F., Corkeron, P.J., Bell, J., Berchok, C., Bonnell, J.M., Thornton, J.B., Brault, S., Buchanan, G.A., Cholewiak, D.M., Clark, C.W., Delarue, J., Hatch, L.T., Klinck, H., Kraus, S.D., Martin, B., Mellinger, D.K., Moors-Murphy, H., Nieukirk, S., Nowacek, D.P., Parks, S.E., Parry, D., Pegg, N., Read, A.J., Rice, A.N., Risch, D., Scott, A., Soldevilla, M.S., Stafford, K.M., Stanistreet, J.E., Summers, E., Todd, S., Parijs, S.M.V., 2020. Exploring movement patterns and changing distributions of baleen whales in the western North Atlantic using a decade of passive acoustic data. Glob. Change Biol. 26, 4812–4840.

Delarue, J., Laurinolli, M., Martin, B., 2009. Bowhead whale (*Balaena mysticetus*) songs in the Chukchi Sea between October 2007 and May 2008. J. Acoust. Soc. Am. 126, 3319–3328.

Dobrev, I., Sim, J.H., Stenfelt, S., Ihrle, S., Gerig, R., Pfiffner, F., Eiber, A., Huber, A.M., Roosli, C., 2017. Sound wave propagation on the human skull surface with bone conduction stimulation. Hear. Res. 355, 1–13.

Dunlop, R.A., 2018. The communication space of humpback whale social sounds in wind-dominated noise. J. Acoust. Soc. Am. 144, 540–551.

Edds-Walton, P.L., 1997. Acoustic communication signals of Mysticete whales. Bioacoustics 8, 47–60.

Erbe, C., Marley, S.A., Schoeman, R., Smith, J.N., Trigg, L.E., Embling, C., 2019. The effects of ship noise on marine mammals—a review. Front. Mar. Sci. 6.

Escobar, I., 2016. Sound reception mechanism analysis of a Cuvier's beaked whale (*Ziphius cavirostris*),. *Struct. Eng.* (Univ. California, San Diego, San Diego) 59.

Ewing, M., Worzel, J.L., 1948. Long-range sound transmission. Geol. Soc. Am. Mem. 27, 1–32.

Fleischer, G., 1980. Low-frequency receiver of the middle ear in mysticetes and odontocetes. In: Busnel, R.G., Fish, J.F. (Eds.), Animal Sonar Systems. Plenum Publishing Corporation, New York, pp. 891–893.

Frankel, A.S., Clark, C.W., 1998. Results of low-frequency m-sequence noise playbacks to humpback whales in Hawai`i. Can. J. Zool. 76, 521–535.

Frankel, A.S., Stein, P.J., 2020. Gray whales hear and respond to signals from a 21-25kHz active sonar. Marine Mammal Sci. 36, 1111–1125.

Frasier, T.R., Koroscil, S.M., White, B.N., Darling, J.D., 2011. Assessment of population substructure in relation to summer feeding ground use in the eastern North Pacific gray whale. Endanger. Species Res. 14, 39–48.

Gedamke, J., Costa, D.P., Dunstan, A., 2001. Localization and visual verification of a complex minke whale vocalization. J. Acoust. Soc. Am. 109, 3038–3047.

Groves, S.L., Peredo, C.M., Pyenson, N.D., 2021. What are the limits on whale ear bone size? Non-isometric scaling of the cetacean bulla. PeerJ 9.

Helble, T., Alongi, G., Guazzo, R., Allhusen, D., Martin, C., Martin, S., Durbach, I., Henderson, E., 2024. Swimming and acoustic calling behavior attributed to Bryde's whales in the central North Pacific. Front. Mar. Sci. 11.

Herr, H., Viquerat, S., Devas, F., Lees, A., Wells, L., Gregory, B., Giffords, T., Beecham, D., Meyer, B., 2022. Return of large fin whale feeding aggregations to historical whaling grounds in the Southern Ocean. Sci. Rep. 12.

Hickling, R., Wang, N.M., 1966. Scattering of sound by a rigid movable sphere. J. Acoust. Soc. Am. 39, 276–279.

Hood, J.D., 2005. Bone conduction: a review of the present position with especial reference to the contributions of Dr. Georg von Békésy. J. Acoust. Soc. Am. 34, 1325–1332.

Kellogg, R., 1928. The History of Whales-Their Adaptation to Life in the Water (Concluded). Q. Rev. Biol. 3, 174–208.

Kleivane, L., Kvadsheim, P.H., Vinje, A.V.P., Mulsow, J., Ølberg, R.A., Teilmann, J., Harms, C., Houser, D., 2024. Capture and release of minke whales offers new research opportunities, including measurements of mysticete hearing. Aquat. Mamm. 50, 352–368.

Krysl, P., Cranford, T.W., 2016. Directional hearing and head-related transfer function in Odontocete Cetaceans. In: Popper, A.N., Hawkins, A.D. (Eds.), Effects of Noise on Aquatic Life II. Springer Science+Business Media, New York, pp. 583–587.

Krysl, P., Cranford, T.W., Wiggins, S.M., Hildebrand, J.A., 2006. Simulating the effect of high-intensity sound on cetaceans: modeling approach and a case study for Cuvier's beaked whale (*Ziphius cavirostris*). J. Acoust. Soc. Am. 120, 2328–2339.

Krysl, P., Hawkins, A.D., Schilt, C., Cranford, T.W., 2012. Angular oscillation of solid scatterers in response to progressive planar acoustic waves: do fish Otoliths rock? *PLoS One* (Public Lib. Sci.), e42591.

Kvadsheim, P.H., DeRuiter, S., Sivle, L.D., Goldbogen, J., Roland-Hansen, R., Miller, P.J.O., Lam, F.-P.A., Calambokidis, J., Friedlaender, A., Visser, F., Tyack, P.L., Kleivane, L., Southall, B., 2017. Avoidance responses of minke whales to 1-4kHz naval sonar. Mar. Pollut. Bull. 121, 60–68.

Lancaster, W.C., Ary, W.J., Krysl, P., Cranford, T.W., 2015. Precocial Development within the Tympanoperiotic Complex in Cetaceans. Mar. Mamm. Sci. 31, 369–375.

Lillie, D.G., 1910. Observations on the anatomy and general biology of some members of the larger Cetacea. Proc. Zool. Soc. Lond. 80, 769–792.

Lockyer, C., 1976. Body weights of some species of large whales. J. Cons. Int. Explor. Mer. 36, 259–273.

McDonald, M.A., Hildebrand, J.A., Webb, S.C., 1995. Blue and fin whales observed on a seafloor array in the Northeast Pacific. J. Acous. Soc. Am. 98, 712–721.

McDonald, M.A., Mesnick, S.L., Hildebrand, J.A., 2006. Biogeographic characterization of blue whale song worldwide: using song to identify populations. J. Cetacean Res. Manag. 8, 55–65.

McKenna, M.F., Calambokidis, J., Oleson, E.M., Laist, D.W., Goldbogen, J.A., 2015. Simultaneous tracking of blue whales and large ships demonstrates limited behavioral responses for avoiding collision. Endanger. Species Res. 27, 219–232.

Mobley Jr, J.R., Herman, L.M., Frankel, A.S, 1988. Responses of wintering humpback whales (*Megaptera novaeangliae*) to playback of recordings of winter and summer vocalizations and of synthetic sound. Behav. Ecol. Sociobiol. 23, 211–223.

Morris, M., Krysl, P., Hildebrand, J., Cranford, T., 2023. Resonance of the tympanoperiotic complex of fin whales with implications for their low frequency hearing. PLoS ONE 18.

Morris, M., Krysl, P., Hildebrand, J., Cranford, T., 2025. Experimental observations of gray whale skull vibrations amplified in the bony hearing complex. Sci Rep 15.

Narins, P.M., Lewis, E.R., 1984. The vertebrate ear as an exquisite seismic sensor. J. Acoust. Soc. Am. 76, 1384–1387.

Nishiwaki, M., 1950. The body weight of whales. Sci. Rep. Whales Res. Inst. 4, 184–209.

Norris, K.S., Goodman, R.M., Villa-Ramirez, B., Hobbs, L., 1977. The behavior of California Gray Whales (*Eschrichtius robustus*) in Southern Baja California, Mexico. Fishery Bulletin 75, 159–172.

Nowacek, D.P., Johnson, M.P., Tyack, P.L., 2004. North Atlantic right whales (*Eubalaena glacialis*) ignore ships but respond to alerting stimuli. Proc. R. Soc. B 271, 227–231.

Nowacek, D.P., Thorne, L.H., Johnston, D.W., Tyack, P.L., 2007. Responses of cetaceans to anthropogenic noise. Mamm Rev 37, 81–115.

Parks, S.E., Hamilton, P., Kraus, S., Tyack, P., 2005. The gunshot sound produced by male North Atlantic right whales (Eubalaena glacialis) and its potential function in reproductive advertisement. Marine Mamm. Sci. 21, 458–475.

Payne, K., Payne, R., 1985. Large scale changes over 19 years in songs of humpback whales in Bermuda. Z. Tierpsychol. 68, 89–114.

Payne, R., 1995. Chapter 5 A Heard of Whales. Among Whales. Dell Publishing, New York, pp. 168–211.

Payne, R., Webb, D., 1971. Orientation by means of long range acoustic signaling in baleen whales. Ann. N. Y. Acad. Sci. 188, 110–141.

Payne, R.S., McVay, S., 1971. Songs of the humpback whales. Science 173, 587–597.

Puria, S., 2020. Middle Ear Biomechanics: smooth Sailing. Acoust Today 16, 27–35.

Richardson, W.J., 1995. Marine Mammal Hearing. In: Richardson, W.J., Greene, C.R.J., Malme, C.I., Thomson, D.H. (Eds.), Marine Mammals and Noise. Academic Press, San Diego, pp. 205–240.

Ridgway, S.H., 2000. The auditory central nervous systems of dolphins. In: Au, W.W.L., Popper, A.N., Fay, R.R. (Eds.), Hearing By Whales and Dolphins. Springer-Verlag, New York, pp. 273–293.

Sharpe, F.A., 2001. Social foraging of the southeast Alaskan Humpback whale, *Megaptera novaeangliae*. Prog. Nucl. Energy 6 Biol. Sci. 129.

Širović, A., Hildebrand, J., Wiggins, S., 2007. Blue and fin whale call source levels and propagation range in the Southern Ocean. J. Acoust. Soc. Am. 122, 1208–1215.

Širović, A., Hildebrand, J.A., 2011. Using passive acoustics to model blue whale habitat off the Western Antarctic Peninsula. Deep-Sea Res. II 58, 1719–1728.

Širović, A., Johnson, S.C., Roche, L.K., Varga, L.M., Wiggins, S.M., Hildebrand, J.A., 2014. North Pacific right whales (*Eubalaena japonica*) recorded in the Northeastern Pacific Ocean in 2013. Mar. Mamm. Sci. 31, 800–807.

Širović, A., Williams, L.N., Kerosky, S.M., Wiggins, S.M., Hildebrand, J.A., 2013. Temporal separation of two fin whale call types across the eastern North Pacific. Mar. Biol. 160, 47–57.

Sivle, L.D., Wensveen, P.J., Kvadsheim, P., Lam, F.-P.A., Visser, F., Cure, C., Harris, C.M., Tyack, P.L., Miller, P., 2016. Naval sonar disrupts foraging behaviour in humpback whales. Mar. Ecol. Prog. Ser. 562, 211–220.

Soldevilla, M.S., Debich, A.J., Garrison, L.P., Hildebrand, J.A., Wiggins, S.M., 2022a. Rice's whales in the northwestern Gulf of Mexico: call variation and occurrence beyond the known core habitat. Endanger. Species Res. 48, 155–174.

Soldevilla, M.S., Debich, A.J., Pérez-Carballo, I., Jarriel, S., Frasier, K.E., Garrison, L.P., Gracia, A., Hildebrand, J.A., Rosel, P., Serrano, A., 2024. Rice's whale occurrence in the western Gulf of Mexico from passive acoustic recordings. Mar. Mamm. Sci.

Soldevilla, M.S., Ternus, K., Cook, A., Hildebrand, J.A., Frasier, K.E., Martinez, A., Garrison, L.P., 2022b. Acoustic localization, validation, and characterization of Rice's whale calls. J. Acoust. Soc. Am. 151, 4264–4278.

Southall, B., Berkson, J., Bowen, D., Brake, R., Eckman, J., Field, J., Gisiner, R., Gregerson, S., Lang, W., Lewandoski, J., Wilson, J., Winokur, R., 2009. Addressing the Effects of Human-Generated Sound on Marine Life: An Integrated Research Plan for U.S. federal agencies. Interagency Task Force on Anthropogenic Sound and the Marine Environment of the Joint Subcommittee on Ocean Science and Technology. Washington, DC.

Southall, B.L., Donovan, G.P., Racca, R., Reeves, R.R., Vedenev, A.I., Weller, D.W., 2023. Data collection and analysis methods to evaluate potential impacts of seismic surveys and other marine industrial activities on baleen whales. Ocean Coast. Manag. 245.

Southall, B.L., Nowacek, D.P., Miller, P.J.O., Tyack, P.L., 2016. Experimental field studies to measure behavioral responses of cetaceans to sonar. Endanger. Species Res. 31, 293–315.

Stenfelt, S., 2006. Overview and recent advances in bone conduction physiology. In: Huber, A., Eiber, A. (Eds.), Middle Ear Mechanics in Research and Otology - Proceedings of the 4th International Symposium. World Scientific Publishing Co. Pte. Ltd., Zurich, Switzerland, pp. 1–9.

Stenfelt, S., 2013. Bone conduction and the middle ear. In: Puria, S., Fay, R.R., Popper, A. N. (Eds.), The Middle Ear: Science, Otosurgery, and Technology. Springer, New York, pp. 135–169.

Stimpert, A.K., DeRuiter, S.L., Falcone, E.A., Joseph, J.J., Douglas, A.B., Moretti, D.J., Friedlander, A.S., Calambokidis, J., Gailey, G., Tyack, P.L., Goldbogen, J.A., 2015. Sound production and associated behavior of tagged fin whales (*Balaenoptera physalus*) in the Southern California Bight. Anim. Biotelemetry 3, 1–12.

Stimpert, A.K., Wiley, D.N., Au, W.W.L., Johnson, M.P., Arsenault, R., 2007. Megapclicks": acoustic click trains and buzzes produced during night-time foraging of humpback whales (*Megaptera novaeangliae*). Biol. Lett. 3, 467–470.

Szabo, A., Bejder, L., Warick, H., van, Aswegen, M., Friedlaender, A., Goldbogen, J., Kendall-Bar, J., Leunissen, E., Angot, M., Gough, W., 2024. Solitary humpback whales manufacture bubble-nets as tools to increase prey intake. R Soc Open Sci 11, 1–11.

Tervo, O.M., Christoffersen, M.F., Parks, S.E., Kristensen, R.M., Madsen, P.T., 2011. Evidence for simultaneous sound production in the bowhead whale (*Balaena mysticetus*). J. Acoust. Soc. Am. 130, 2257–2262.

Tervo, O.M., Parks, S.E., Miller, L.A., 2009. Seasonal changes in the vocal behavior of bowhead whales (Balaena mysticetus) in Disko Bay, Western-Greenland. J. Acoust. Soc. Am. 126, 1570–1580.

Thode, A.M., Blackwell, S.B., Conrad, A.S., Kim, K.H., Marques, T., Thomas, L., Oedekoven, C.S., Harris, D., Broker, K., 2020. Roaring and repetition: how bowhead whales adjust their call density and source level (Lombard effect) in the presence of natural and seismic airgun survey noise. J. Acoust. Soc. Am. 147, 2061–2080.

Thompson, T.J., Winn, H.E., Perkins, P.J., Winn, H.E., Olla, B.L., 1979. Mysticete sounds. Behavior of Marine animals: Current Perspectives in Research. Plenum Publishing Corporation, New York and London, pp. 403–431.

Tomilin, A.G., Balaenoptera musculus L. Blue whales, 1967. In: Heptner, V.G. (Ed.), Mammals of the U.S.S.R. and Adjacent Countries. Israel Program for Scientific Translations, Jerusalem, pp. 76–112.

Tonndorf, J., 1972. Bone conduction. In: Tobias, J.V. (Ed.), Bone conduction. Found. Modern Auditory Theory 2, 197–237 edited by Academic Press.

Tyack, P., 1981. Why Do Whales Sing? To keep in touch is only half the answer. Sciences (New York) 21, 22–25.

Tyack, P.L., 1983. Differential response of humpback whales, Megaptera novaeanglia, to playback of song or social sounds. Behav. Ecol. Sociobiol. (Print) 13, 49–55.

Tyack, P.L., 1997. Studying how cetaceans use sound to explore their environment. In: Owings, D.H., MD, B., NS, T. (Eds.), Perspectives in Ethology. Plenum, New York, pp. 251–297.

Tyack, P.L., 2022. Social organization of baleen whales. In: Clark, C.W., Garland, E.C. (Eds.), Ethology and Behavioral Ecology of Mysticetes. Springer Nature, Cham, pp. 147–175.

Tyack, P.L., Zimmer, W.M.X., Moretti, D., Southall, B.L., Claridge, D.E., Durban, J.W., Clark, C.W., D`Amico, A., DiMarzio, N., Jarvis, S., McCarthy, E., Morrissey, R., Ward, J., Boyd, I.L., 2011. Beaked Whales Respond to Simulated and Actual Navy Sonar. PLoS ONE 6.

Varga, L.M., Wiggins, S.M., Hildebrand, J.A., 2018. Behavior of singing fin whales *Balaenoptera physalus* tracked acoustically offshore of Southern California. Endanger. Species Res. 35, 113–124.

Watkins, W.A., 1981. Activities and underwater sounds of fin whales. Sci. Rep. Whales Res. Inst. 33, 83–117.

Watkins, W.A., Daher, M.A., George, J.E., Rodriguez, D., 2004. Twelve years of tracking 52-Hz whale calls from a unique source in the North Pacific. Deep-Sea Res., Instrum. Methods 51, 1889–1901.

Webb, D.C., Tucker, M.J., 1970. Transmission characteristics of the sofar channel. J. Acoust. Soc. Am. 48, 767–769.

Weirathmueller, M., Wilcock, W., Soule, D., 2013. Source levels of fin whale 20 Hz pulses measured in the Northeast Pacific Ocean. J. Acoust. Soc. Am. 133, 741–749.

Wiley, D., Ware, C., Bocconcelli, A., Cholewiak, D., Friedlaender, A., Thompson, M., Weinrich, M., 2011. Underwater components of humpback whale bubble-net feeding behaviour. Behaviour 148, 575–602.

Winn, H.E., Perkins, P.J., 1976. Distribution and sounds of the minke whale, with a review of mysticete sounds. Cetology 19, 1–12.

Yamato, M., Ketten, D.R., Arruda, J., Cramer, S., Moore, K., 2012. The auditory anatomy of the minke whale (*Balaenoptera acutorostrata*): a potential fatty sound reception pathway in a baleen whale. Anat. Rec. 295, 991–998.

Zhu, J., Wen, L., 2024. Hydroacoustic study of fin whales around the Southern Wake Island: type, vocal behavior, and temporal evolution from 2010 to 2022. J. Acoust. Soc. Am. 155, 3037–3050.